



Contents lists available at ScienceDirect

Journal of King Saud University – Science

journal homepage: www.sciencedirect.com

Original article

Landslide susceptibility assessment and their disastrous impact on Makkah Al-Mukarramah urban Expansion, Saudi Arabia, using microtremor measurements

Kamal Abdelrahman^{a,b}, Naif Al-Otaibi^a, Elkhedr Ibrahim^a, Abdullah Binsadoon^{a,*}^a Department of Geology & Geophysics, College of Science, King Saud Univ., P.O. Box 2455, Riyadh 11451, Saudi Arabia^b Department of Seismology, National Research Institute of Astronomy and Geophysics (NRIAG), Helwan 11722, Cairo, Egypt

ARTICLE INFO

Article history:

Received 22 February 2021

Revised 24 March 2021

Accepted 12 April 2021

Available online 22 April 2021

Keywords:

Microtremors

Landslide

Resonance frequency

Directional resonance

Makkah Al-Mukarramah

Saudi Arabia

ABSTRACT

Landslide susceptibility of Makkah Al-Mukarramah has been assessed by collecting microtremor measurements at 277 sites covering the whole area. These data were then processed and analyzed using the horizontal-vertical spectral ratio (HVSr) method to obtain the resonance frequency and H/V amplification factor. The results display that the predominant frequency values range between 0.26 and 17.27 Hz, and the amplification factor varies from 0.87 to 14.68. Then, 34 sites were selected to assess the frequency, amplitude and azimuthal site response where frequency ranges from 0.26 to 13.67 Hz while amplitude varies from 2.0 to 12.2. Moreover, the site response direction was parallel to the landslide directional response in the sliding areas which indicates that the site response direction followed the landslide direction. The results of this study have been approved practically at several sites through field measurements at some of recent landslide occurrence locations in Makkah urban area. These results signifying that microtremor measurements are effective technique in locating the sites suffering landslides, which, in turn, reduce their hazardous impact on either human-life and their beings. Therefore, it is highly recommended to apply this approach in places prone to landslides in southwestern Saudi Arabia.

© 2021 The Author(s). Published by Elsevier B.V. on behalf of King Saud University. This is an open access article under the CC BY-NC-ND license (<http://creativecommons.org/licenses/by-nc-nd/4.0/>).

1. Introduction

The Makkah Al-Mukarramah urban area is bounded by rugged topography and steep-slope mountainous heights in the southwest of Saudi Arabia (Fig. 1). This mountainous location has defined the city's contemporary expansion. The urban communities and facilities are extended through low-land zones, where the Al-Haram area is lower than most of the city. The area around the mosque consists of old structures and is built on the edges of steep-slope hilly blocks. Traditional homes are built from local rock. Rainfall in Makkah flows from the higher edges along the natural slopes. If these slopes are close to the main roads, it will be more vulner-

able. The density of population is high, where permanent residents living along the natural slopes of the Old City. Moreover, the huge visitors of the city for the yearly-round pilgrimage.

Number of major earthquakes affected Makkah on the October 8, 1992, Al-Sharai'a earthquake; the September 12, 2005, non-tectonic seismic shock; and recently, the November 28, 2019 earthquake. These earthquakes affected most of the area, with great ground motion and a hazardous impact (Abdelrahman et al., 2019a, 2019b). In addition, the potentially active tectonic structures that surround the city will increase the susceptibility of landslide phenomenon where it acts as more vulnerable locations.

The disastrous impacts of landslide are readily acknowledged and intensively investigated by several authors worldwide (Saputra et al., 2016; Shanmugam and Wang, 2015; Aleotti and Chowdhury, 1999; Al-Saud, 2015; Youssef et al., 2015a, 2015b, 2015c; Mora and Vahrson, 1994; Mora-Castro et al., 2012; Valenzuela et al., 2018; Berov et al., 2016). Microtremor measurements have been approved at some sites globally by Gaudio and Wasowski (2007), Rezaei et al. (2018), and Zul Bahrum and Sugianto (2018).

Soil response effects, such as resonance frequency and amplification characteristics, are critical for the city of Makkah, where soft

* Corresponding author.

E-mail address: 438106752@student.ksu.edu.sa (A. Binsadoon).

Peer review under responsibility of King Saud University.



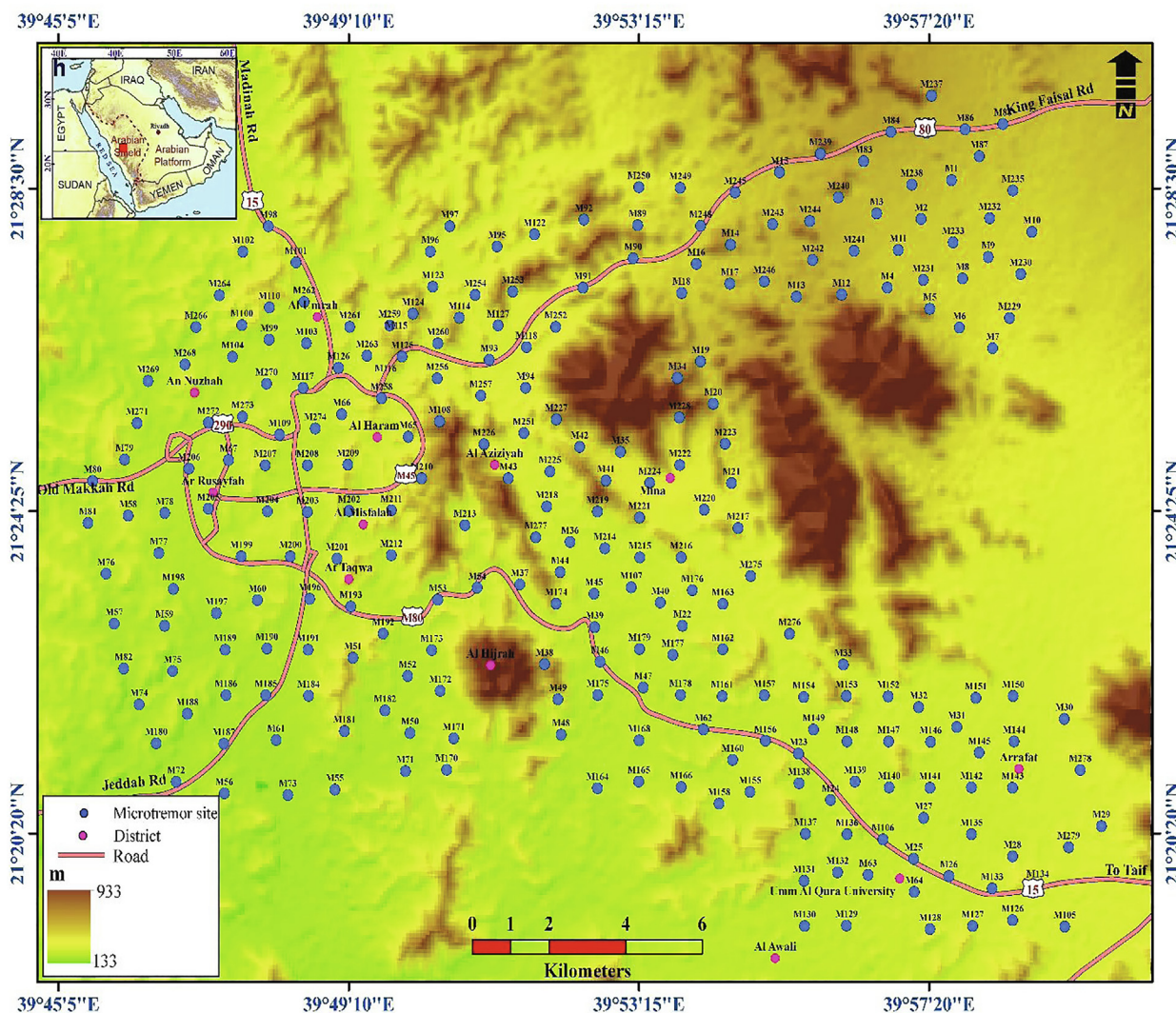


Fig. 1. Location of ambient noise measurements of the study area.

soil, even with small thickness, will accelerate the landslide occurrences, causing huge damage to the population. The closest location of Makkah with an earthquake source zone in the Red Sea permits the efficient transmission of earthquake ground shaking through Makkah. Soft sediments and weathered and cracked blocks will increase the landslide susceptibility. Thus, because of the increasing population, construction, and remarkable economic activities in the area, evaluating the landslide susceptibility of Makkah becomes crucial.

2. Geological settings of Makkah

Geologically, Makkah area comprises Precambrian–Cambrian basement complex, Cretaceous–Tertiary sedimentary sequence, Tertiary–Quaternary basaltic lava flows, and Quaternary–Recent alluvial deposits (Fig. 2). The Precambrian rock units in Makkah have been studied by different authors (e.g. Al-Shanti 1966; Brown et al., 1963; Spincer and Vincent, 1984). The igneous rocks intruded within the metamorphic units, predominantly amphibolite and volcano-sedimentary rocks. Moore and Al-Rehaili (1989) classified

the Precambrian rocks into Late-Proterozoic basaltic to rhyolitic volcanic and volcanoclastic, that have been vaccinated by intrusive bodies of various ages and compositions. Furthermore, intrusions of gabbroic rocks exist. Besides Precambrian dikes related to individual plutons, two types of dikes exist. Mafic dikes consist of gabbroic rocks and ore, dominantly trending east and north-northwest. Moreover, basaltic lava flows covering the upper levels of both the basement complex and the sedimentary rocks. Quaternary deposits distribute in low-land wadies of Makkah area in the form of gravel, alluvial sands of wadi beds with eolian edifices.

Tectonically, Makkah area affected greatly by the Red Sea faulting structures that affected geologic units from the Precambrian to the Quaternary (Sharaf, 2010). Three major fracture trends represent conspicuous geologic structural elements in the region. These fault trends oriented into NW-SE, NE-SW and N-S however, the NW faulting trend is the oldest and represented by normal faults. While, the NE-SW faults dislocate the NW-SE faulting trend forming the second group of faulting. Moreover, the N-S fault trend behave as shear faults with lateral movement for NW-SE and NE-SW faulting trends.

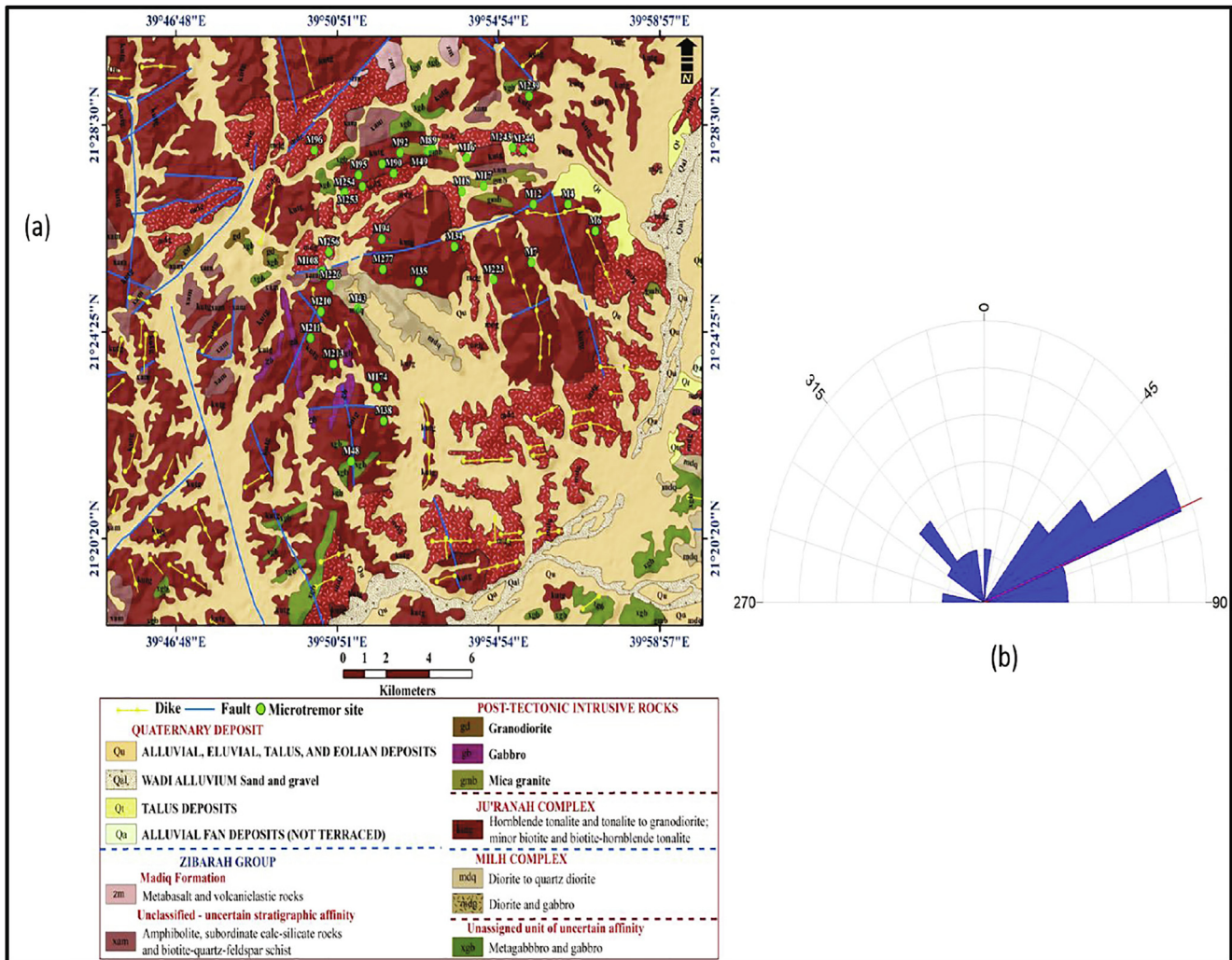


Fig. 2. Geologic setting of Makkah Al-Mukarramah area.

3. Seismicity and seismotectonic setting of Makkah region

Makkah Al-Mukarramah is near the seismically active tectonic environment of the Red Sea (Fig. 3), with potentially active tectonic structures, for example, the Ad-Damm fault zone south of Makkah (Mergelani and Gallanthine 1981). Historical and instrumental earthquake events have occurred in or around the city. Ambraseys et al. (2005) reported several earthquakes occurring in 873, 1121, 1269, 1408, and 1426 CE. Some of these earthquakes caused low to moderate damage to high-rise buildings, for example, minarets and pillars, near the Holy Mosque of Makkah. A detailed earthquake survey of the study area allowed Mergelani and Gallanthine (1981) to detect a series of microearthquakes near Arafat Mountain. Although the location accuracy of these events was small, as they happened outside the survey network, their epicenter could have been in Makkah.

An event that happened on September 28, 1993 (12/4/1413H), confirmed the earthquake vulnerability of Makkah Al-Mukarramah, where the whole city was shaken through earthquake occurring in the Al-Sharai'a district, 30 km northeast of the Holy Mosque. The shock has a magnitude of 3.6 and followed by sequence

of small earthquakes that recorded by seismic network of Saudi Geological Survey. An earthquake swarm has been occurred at Al-Sharai'a on October 3, 1993, a major event with a magnitude of 4.1 Ml (Al-Furaih et al., 1994; Swolfs, 1994). An event with a magnitude of 3.6 was logged close to the same area on June 18, 1994, occurring at the Al Utaibiyya District on 8/8/1426H. This earthquake was predictable and shallow, as suggested by the localized effect.

Fnais et al. (2015) deliberate the seismicity and seismotectonic setting of the Jeddah–Makkah area. They collected historical and instrumentally documented data of earthquakes that affected the Jeddah–Makkah area from various sources and categorized them into a unified earthquake catalog. Five seismotectonic source zones affecting the Makkah region were identified (Fig. 3). Three zones locating in the Red Sea axial trend (northwestern Jeddah, western Jeddah, and southwestern Jeddah zones), whereas two zones lie inland (Thuwal–Rebigh and Jeddah–Makkah zones). It can be stated that the source zone of Jeddah–Makkah is the most susceptible source of the studied area wherever the zone includes tectonic trends. The first one is Wadi Fatima, representing the main fault-bounded graben, 50 km long and 10 km wide. The principle graben of NE-SW has a preexisting faulting trend which separated by NW-SE several faults resulted from the Red Sea major tectonics

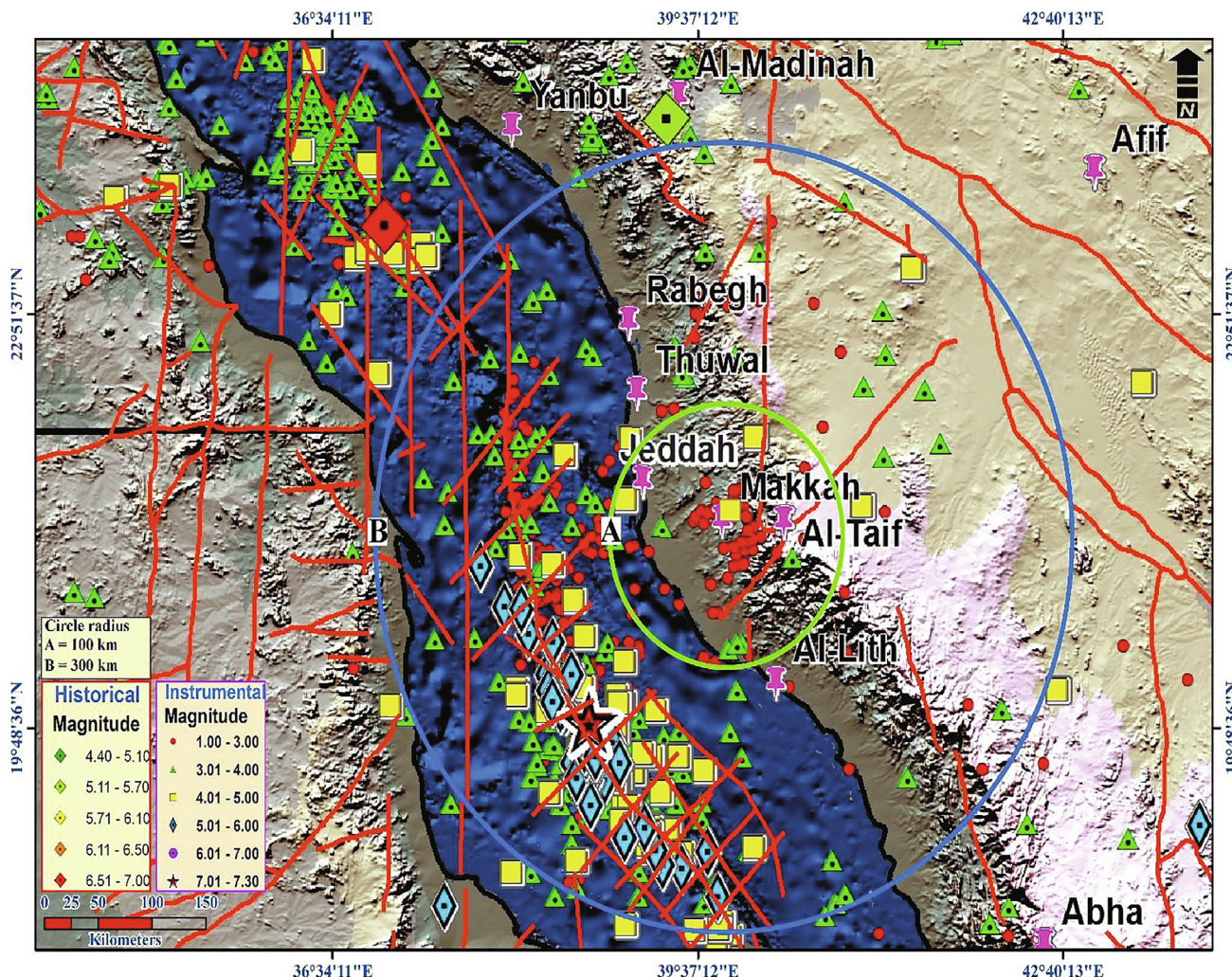


Fig. 3. Seismicity and seismotectonic setting of the Makkah area.

(Al-Garni, 2009). The NNE fractures indicate that the area belongs to a conjugate set of tertiary ruptures. The path of Wadi Fatima spreads ENE-WSW to the south of the city of Jeddah. It abruptly diverts northward, possibly because of active faults (Azzedine et al., 1998). The secondary trend is the Ad-Damm active fault, a major fault trend positioned in the Jeddah–Makkah area.

4. Microtremor measurements

The study area comprised 277 sites for microtremor measurements (Fig. 1). The data collection experimental parameters followed the recommendations of the SESAME team (SESAME 2004). Microtremors were measured for at least 1 h at each site to guarantee long records free from transient conflicts (e.g., moving vehicles and wind gusts) using STA/LTA anti-trigger algorithm. Data were monitored by a sampling rate of 100 sps and filtered using a 0.2–20 Hz bandpass filter. The seismometers were calibrated before recording, installed in good coupling with the surficial soil, oriented horizontally (N–S and E–W), and leveled vertically. The quality and precision of the results attained using this method depend on the processing sequence. In this research, Geopsy software was used to process the records (Wathelet, 2006). The results of microtremor have been verified using the SESAME team’s standards for the reliability. Moreover, the site response direction was assessed using the

azimuthal rotation of the horizontal to vertical spectral ratio with intervals of 10° azimuth.

5. Results and discussion

5.1. Estimation of predominant frequency and H/V amplitude

Microtremor records were processed and their H/V spectral ratios calculated using the steps described above (Fig. 4). The predominant frequency and H/V amplitude were estimated using the spectral ratios of H/V readings. Table 1 shows the resonance frequency and H/V amplitude values for different stations where both f_0 and A_0 represent the observed predominant frequency and H/V amplitude for every station, respectively. The H/V spectral ratios were examined in the processing sequence through SESAME criteria at 277 stations. Explaining these criteria is beyond the scope of the SESAME guidelines (SESAME, 2004).

Investigating the condition of the ground confirmed these results. Thus, the correctness of the results was approved at these stations. To confirm such a conclusion, measurements were conducted at these stations again, obtaining comparable results revealing the maximum and minimum predominant frequencies for Makkah area were 0.26 and 17.27 Hz, respectively. The maximum and minimum amplitudes equalled 0.87 and 14.68, respectively.

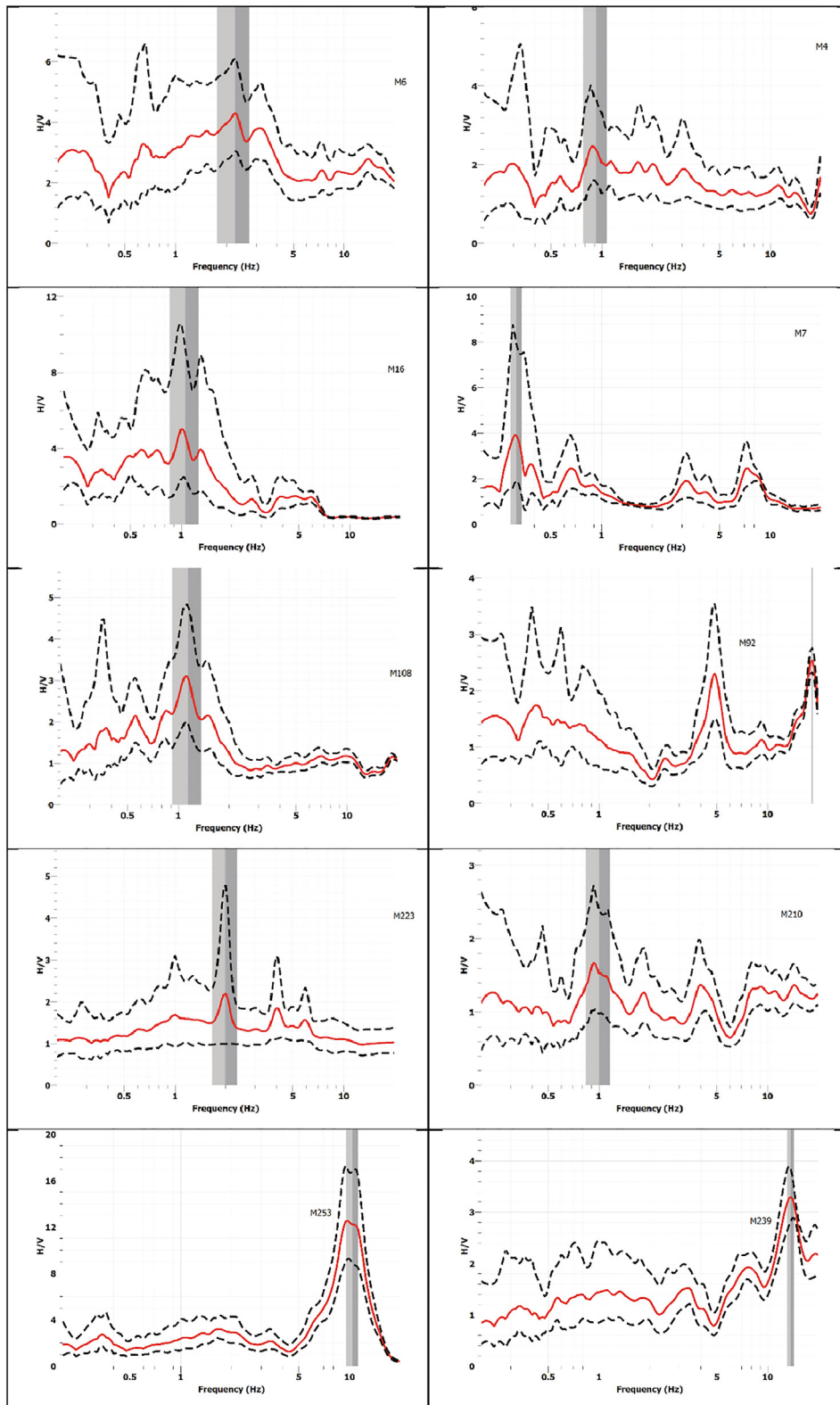


Fig. 4

Fig. 4. Examples of H/V spectral ratio at ambient noise measurement stations.

Table 1
Direction of site response at ambient noise measurement stations.

Site No.	Longitude	Latitude	F ₀	A ₀	Azimuth (°)
M4	39.9441	21.44895	0.93	2.53	35
M6	39.95555	21.44017	3.16	4.22	100
M7	39.92871	21.42987	0.67	2.58	80
M12	39.92964	21.44896	1.11	2.4	40
M16	39.90162	21.46418	1.04	5.51	20
M17	39.90883	21.45493	1.33	2.93	120
M18	39.89962	21.45315	0.66	2.82	160
M34	39.89655	21.43507	0.68	3.26	70
M35	39.88169	21.42351	0.92	3.1	130
M38	39.86686	21.37764	1.11	3.29	30
M43	39.85615	21.41448	1.01	2.9	20
M48	39.85329	21.36435	0.87	2	140
M49	39.887189	21.46729	1.13	12.01	10
M89	39.88568	21.46648	0.97	2.76	150
M90	39.8711	21.45911	2.34	2.33	40
M92	39.87378	21.46589	4.88	2.32	80
M94	39.86607	21.4375	0.8	4.48	120
M95	39.85644	21.45859	0.82	3.86	60
M96	39.83785	21.4667	6.24	2.06	30
M108	39.84106	21.42696	1.07	2.39	140
M122	39.86627	21.46226	1.33	2.21	80
M174	39.86417	21.38861	5.6	4.67	10
M210	39.84062	21.41363	0.45	2.58	140
M211	39.83629	21.40492	1.95	2.34	60
M213	39.84582	21.39638	1.07	3.82	80
M223	39.91296	21.42417	2.02	2.3	120
M226	39.8445	21.42237	1.01	3.51	40
M239	39.92783	21.48449	13.67	3.11	65
M243	39.92098	21.46762	0.68	4.69	110
M244	39.92547	21.46708	0.61	6.71	60
M253	39.85805	21.45484	10.28	12.2	90
M254	39.85054	21.45281	13.01	8.17	30
M256	39.84393	21.4332	11.24	5.33	160
M277	39.8666	21.42754	0.26	2.13	115
					10
					160

The high values of the fundamental frequency indicate a seismic impedance contrast in the shallow interface. The microtremor measurement results were presented in the form of a zonation map for further interpretation. ArcGIS software was used to draw the maps. The interpolation of the results was obtained using ambient noise measurements. Fig. 5 represents zoning map for predominant frequency while Fig. 6 shows the H/V amplitude zonation map.

5.2. Estimation the direction of site response

As indicated before, the response direction has been assessed through the rotation at azimuth intervals of 10° of the H/V spectral ratio. The site response direction was evaluated using the three quantities of frequency, amplitude, and azimuth. Fig. 7 illustrates the H/V spectral rotation ratio at various stations. The analysis of these data illustrates that the frequency values span between 0.26 and 13.67 Hz while amplitude extends from 2.0 to 12.2. This figure proves that 34 stations show directivity (Fig. 8). It is noticed that, for these stations, the H/V amplification arises in a specific

direction reflecting the impact of the integration between the localized site response, geometrical and the geologic circumstances.

Moreover, the directivity is evident at stations on the landslide sites. Such explanations in agreement with Panzera et al. (2011), Del Gaudio and Wasowski (2014), and Pilz et al. (2014). Table 1 shows the site response direction at 34 stations.

Several field tests and measurements were conducted at some landslide locations of Makkah Al-Mukarramah. Significant efforts were made to identify all slide paths and old landslides through the field survey to find a proper interpretation of the results. Fig. 9 shows examples of this field survey, proving that stations exhibiting directivity were on landslide sites. A more detailed examination indicates that stations with directivity followed the landslide direction. It is noticed that, the maximum slope follows the landslide direction in the sliding areas. These results correlated with that of Burjanek et al. (2010); Panzera, Lombardo, and Rigano (2011); Del Gaudio, Muscillo, and Wasowski (2014); and Pilz et al. (2014).

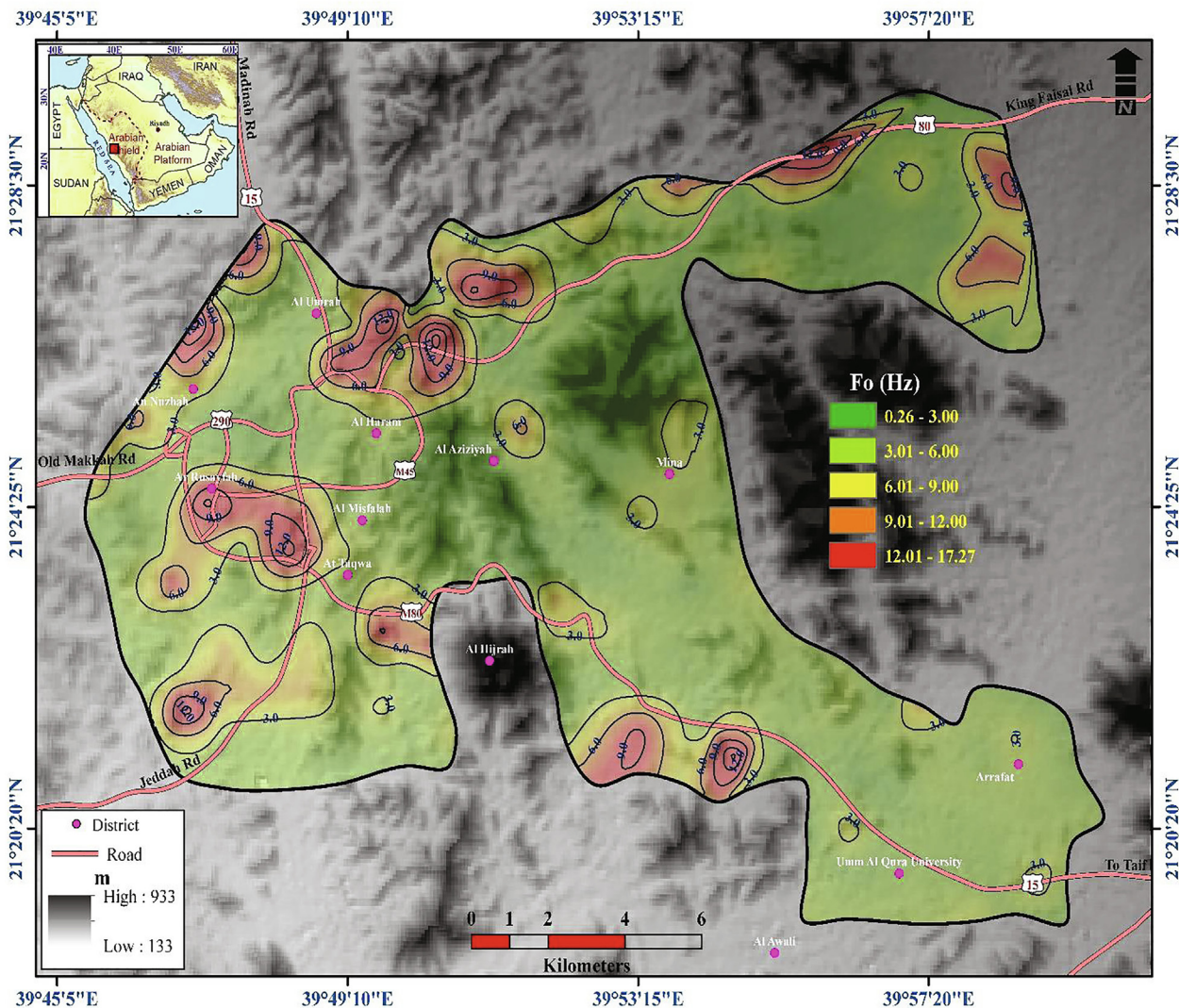


Fig. 5. Fundamental frequency zonation map.

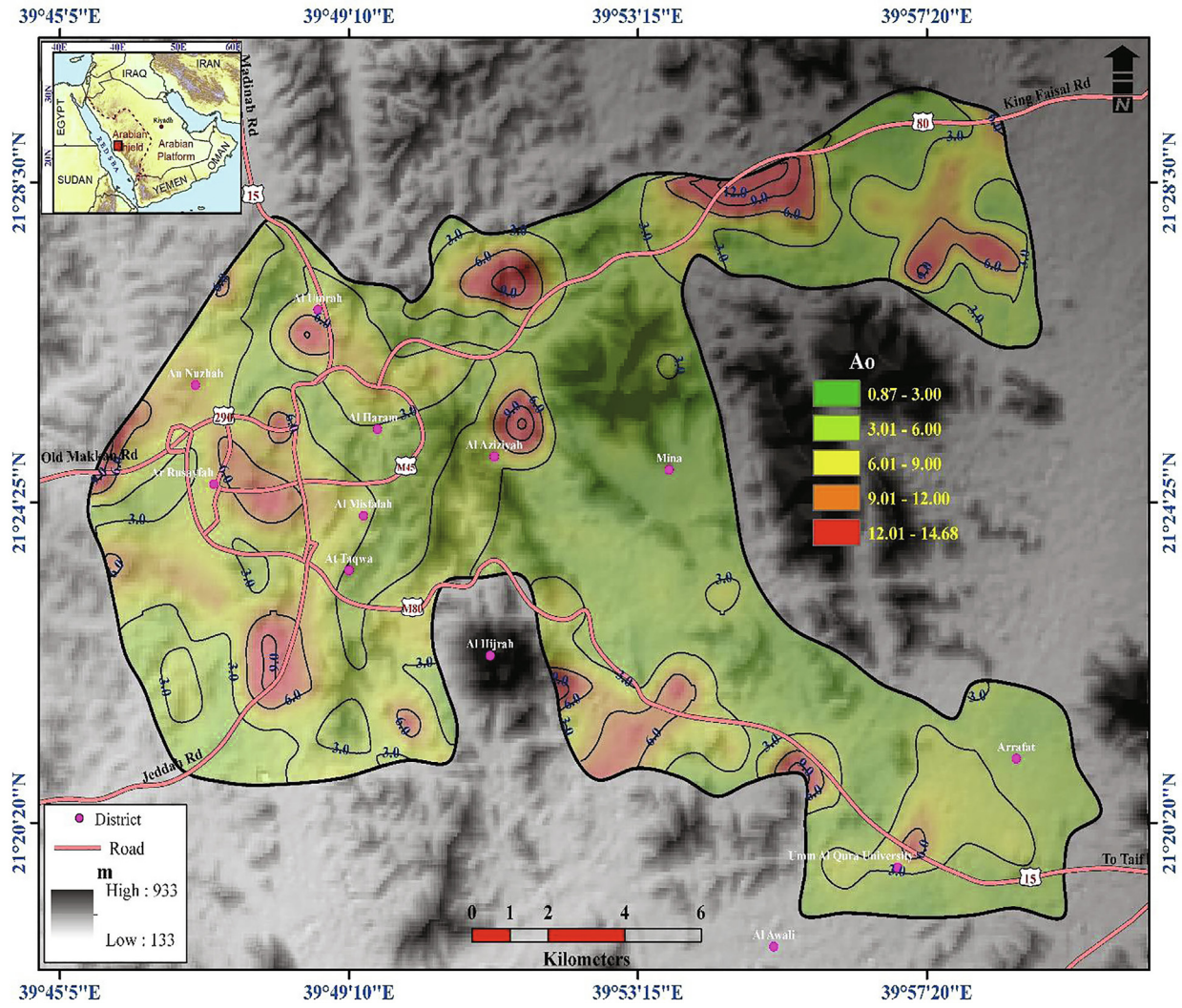


Fig. 6. The H/V amplitude zonation map.

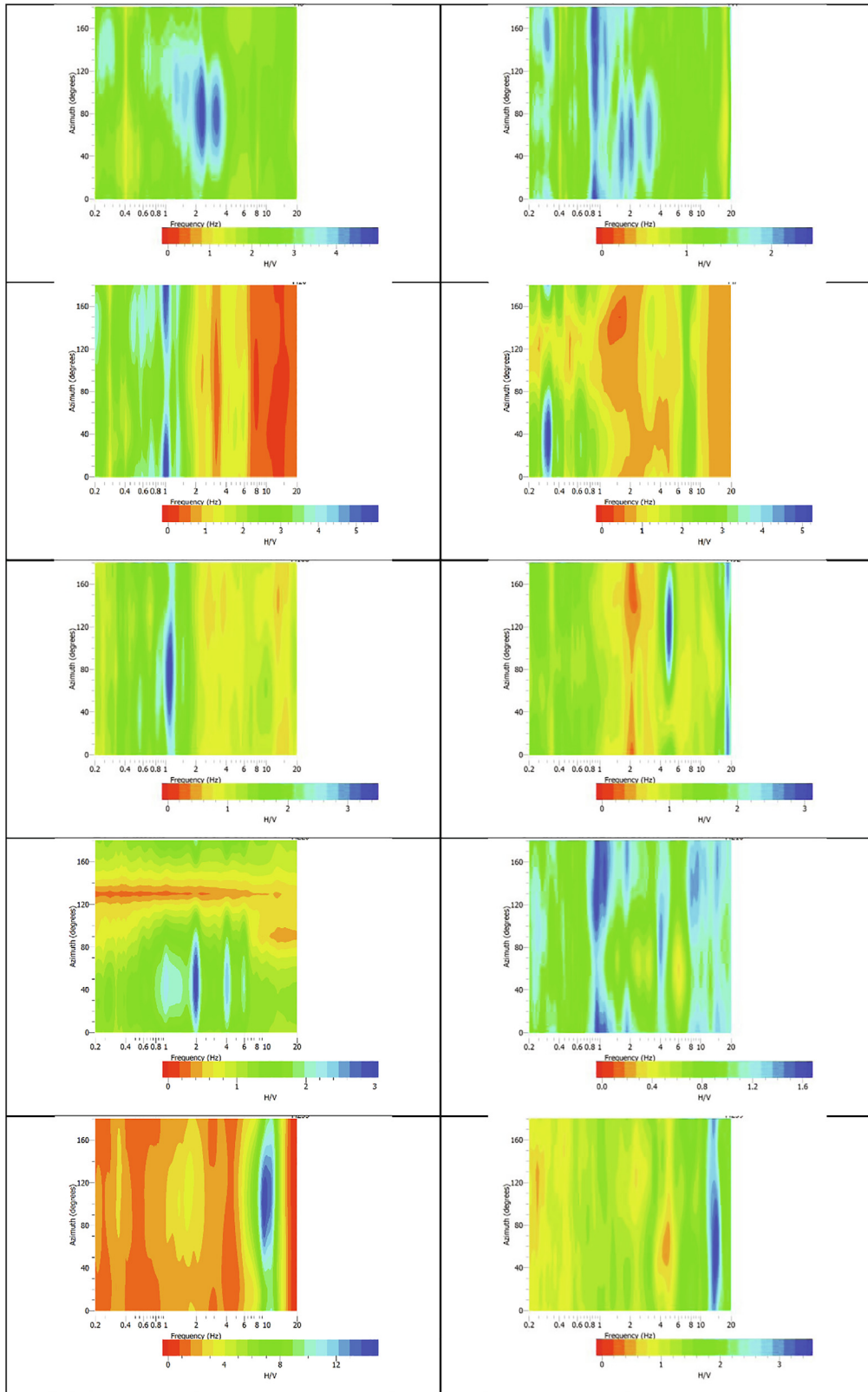


Fig. 7. Examples of H/V spectral ratio rotation at microtremor measurement stations.

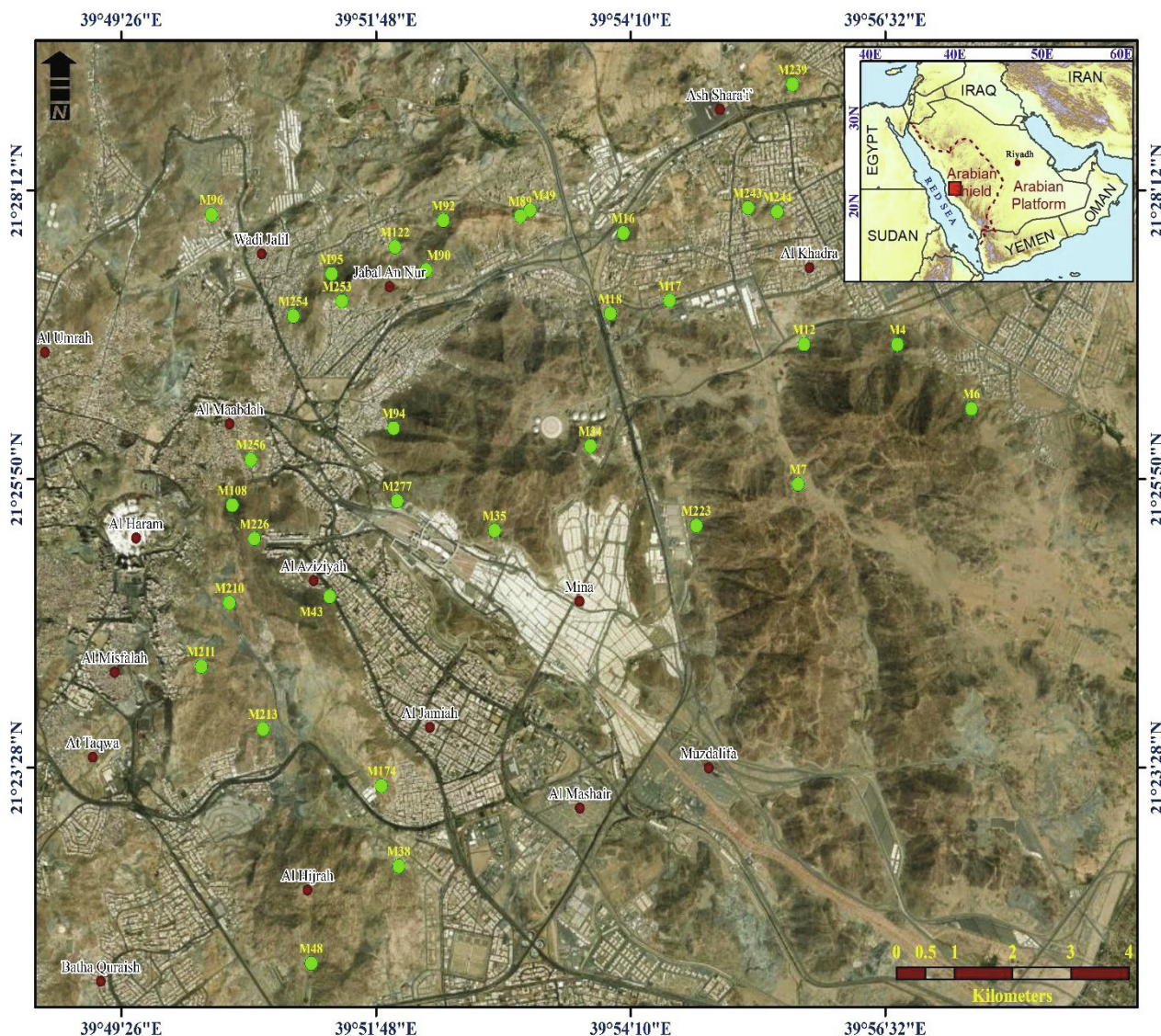


Fig. 8. The selected sites for site response directivity measurements.

6. Conclusions

In this study, microtremor measurements were conducted at 277 stations to estimate landslide susceptibility of the Makkah Al-Mukarramah. The processed data through Nakamura technique in order to obtain the predominant frequency, H/V amplitude. Then, mapping of these parameters through Makkah investigated area. The verification of the directional site response phenomenon was measured by the rotation in azimuth intervals of 10° of the H/V spectral ratios. Then, the directivity results were verified with a field survey to evaluate the accuracy of the microtremor measurements.

These results clarified both of maximum and minimum predominant frequencies throughout Makkah were 6.86 and 3.34 Hz, respectively. The maximum and minimum H/V ampli-

tudes equaled 3.34 and 2.01, respectively. The high values of the fundamental frequency indicate a seismic impedance contrast in the shallow interface. Directivity was obvious at stations in the landslide area. A detailed inspection of microtremor stations indicated that the site response directions were parallel to the main direction of landslide. According to these results, the microtremor measurements provide a comprehensive approach to landslide assessment. It reduces the initial costs of numerical analyses and accelerates landslide analyses.

Declaration of Competing Interest

The authors declare that they have no known competing financial interests or personal relationships that could have appeared to influence the work reported in this paper.

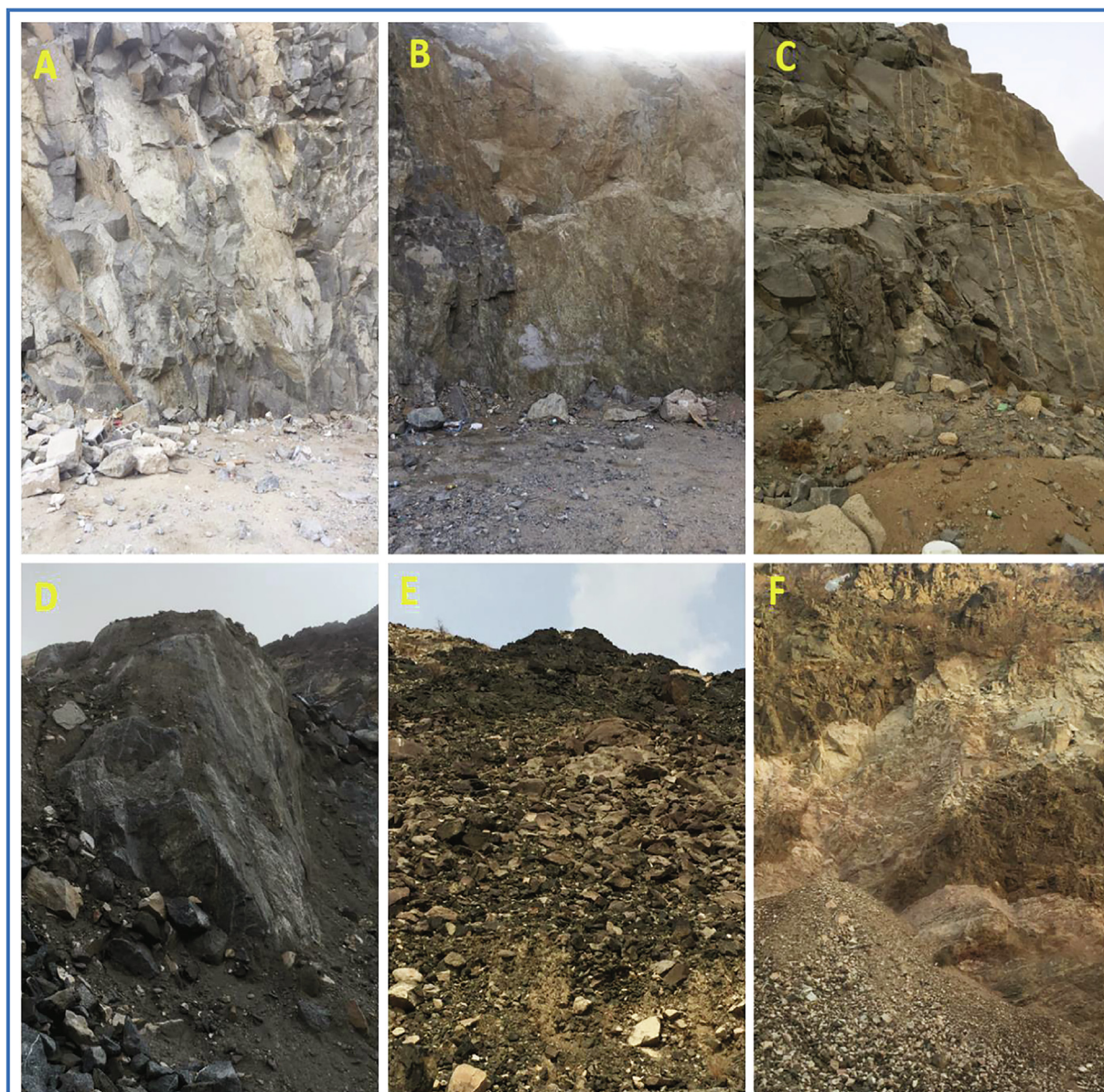


Fig. 9. Landslide field verification sites.

Acknowledgments

The authors extend their appreciation to the Deanship of Scientific Research at King Saud University for funding this work through the research group No. RGP -1436-011.

References

- Abdelrahman, K., Al-Amri, A., Al-Otaibi, N., Fnais, M., Abdelmonem, E., 2019a. Ground motion acceleration and response spectra of Al-Mashair area, Makkah Al-Mukarramah, Saudi Arabia. *Arabian J. Geosci.* 12 (11), 346.
- Abdelrahman, K., Al-Amri, A.M., Al-Otaibi, N.A., Fnais, M., Abdelmonem, E., 2019b. Seismic hazard assessment of al Mashair area, Makkah Al-Mukarramah (Saudi Arabia). In: *On Significant Applications of Geophysical Methods*. Springer, pp. 227–230.
- Al-Saud, M., 2015. Seismic characteristics and kinematic models of Makkah and central red sea regions. *Arabian J. Geosci.* 1 (1), 49–61.
- Aleotti, P., Chowdhury, R., 1999. Landslide hazard assessment: summary review and new perspectives. *Bull. Eng. Geol. Environ.* 58 (1), 21–44.
- Al-Furaih, A.A., Al-Aswad, A.A., Kebeasy, R.M., 1994. New Aspects on Estimated Risk around the Makkah Region. 2nd Ann. Meeting of Saudi. Soc. Earth Sci. 19, 25–27.
- Al-Garni, M., 2009. Geophysical Investigations for Groundwater in a Complex Subsurface Terrain, Wadi Fatima, KSA: A Case History. *Jordan J. Civ. Eng.* 3 (2), 118–136.
- Ambraseys, N.N., Melville, C.P., Adams, R.D., 2005. *The seismicity of Egypt, Arabia and the Red Sea: a historical review*. Cambridge University Press.
- Berov, B., Ivanov, P., Dobrev, N., Krastanov, M., 2016. Addition to the method of mora & vahrson for landslide susceptibility along the Bulgarian black seacoast. CRC Press, Napoli, Italy.
- Burjanek, J., G. Gassner-Stamm, V. Poggi, J. R. Moore, and D. Fah. 2010. "Ambient Vibration Analysis of an Unstable Mountain Slope." *Geophysical Journal International* 180: 820–828.
- Del Gaudio, V., Muscillo, S., Wasowski, J., 2014. What we can learn about slope response to earthquakes from ambient noise analysis: an overview. *Eng. Geol.* 182, 182–200.
- Azzedine, B., Ritz, J., Philip, H., 1998. Drainage Diversions as Evidence of Propagating Faults: example of the El Asnam and Thenia Faults, Algeria. *Terra Nova* 10, 236–244.
- Fnais, M., Al-Amri, A., Abdelrahman, K., Abdelmonem, E., El-Hady, S., 2015. Seismicity and seismotectonic of Jeddah-Makkah region, west-central Saudi Arabia. *J. Earth Sci.* 26 (5), 746–754.
- Gaudio, V.D., Wasowski, J., 2007. Directivity of slope dynamic response to seismic shaking. *J. Geophys. Res. Lett.* 34, 2007.
- Merghealani, H.M., Gallanthine, S.K., 1981. Microearthquakes in the Tihamat-Asir Region of Saudi Arabia. *Bull. Seism. Soc. Am.* 70 (6), 2291–2293.

- Moore, T. and Al-Rehaili, M. (1989). Geologic map of the Makkah quadrangle, sheet 21d. Kingdom of Saudi Arabia, Saudi Arabian Directorate General of Mineral Resources Geoscience Map GM-107C, scale, 1(250,000).
- Mora, C., S. and Vahrson, W.-G. (1994). Macrozonation methodology for landslide hazard determination. *Bulletin of the Association of Engineering Geologists*, 31 (1):49–58.
- Mora-Castro, S., Saborio, J., Asté, J., Prepetit, C., Joseph, V., and Matera, M. (2012). Slope instability hazard in Haiti: Emergency assessment for a safe reconstruction. *Landslides and Engineered Slopes: Protecting Society through Improved Understanding*. Taylor & Francis Group, London, pages 153–172.
- Panzer, F., Lombardo, G., Rigano, R., 2011. Evidence of topographic effects through the analysis of ambient noise measurements. *Seismol. Res. Lett.* 82, 413–419.
- Pilz, M., Parolai, S., Bindi, D., Saponaro, A., Abdybachev, U., 2014. Combining seismic noise techniques for landslide characterization. *Pure Appl. Geophys.* 171, 1729–1745.
- Rezaei, S., Issa, Sh., Hamed, R., 2018. Evaluation of landslides using ambient noise measurements (case study: Nargeschal landslide). *Int. J. Geotech. Eng.* <https://doi.org/10.1080/19386362.2018.1431354>.
- Saputra, A., Gomez, C., Hadmoko, D.S., Sartohadi, J., 2016. Coseismic landslide susceptibility assessment using geographic information system. *Geoenviron. Disasters* 3 (1), 27.
- Shanmugam, G., Wang, Y., 2015. The landslide problem. *J. Palaeogeogr.* 4 (2), 109–166.
- Sharaf, M.A., 2010. Geological and geophysical exploration of the groundwater aquifers of As Suqah area, Makkah district, Western Arabian Shield. *Saudi Arabia. Arab. J. Geosci* 2011 (4), 993–1004. <https://doi.org/10.1007/s12517-010-0187-1>.
- Swolfs, H. S., 1994. Listing of Earthquakes in the Arabian Tectonic Plate. USGS-DFR-94-3.29
- Youssef, A., Pradhan, B., Al-Kathery, M., Bathrellos, G., Skilodimou, H., 2015. Assessment of rockfall hazard at Al-Noor mountain, Makkah city (Saudi Arabia) using spatio-temporal remote sensing data and field investigation. *J. Afr. Earth Sc.* 101, 309–321.
- Youssef, A., Pradhan, B., Pourghasemi, H., Abdullahi, S., 2015b. Landslide susceptibility assessment at wadi Jawrah basin, Jizan region, Saudi Arabia using two bivariate models in GIS. *Geosci. J.* 19 (3), 449–469.
- Zul Bahrum, S., Sugianto, N., 2018. Geological condition at landslides potential area based on Microtremor survey. *ARPJ. Eng. Appl. Sci.* 13 (8), 3007–3013.